

Supporting Information

Post-synthetic π -extension of perylene conjugated porous polymer via APEX reactions: Tunable optical and gas storage properties

1. General methods.....	S2
2. Computational Details.....	S3
2. Synthesis.....	S4
3. Supporting figures and tables.....	S7
4. References.....	S25
5. Optimized geometry.....	S26

1. General Methods:

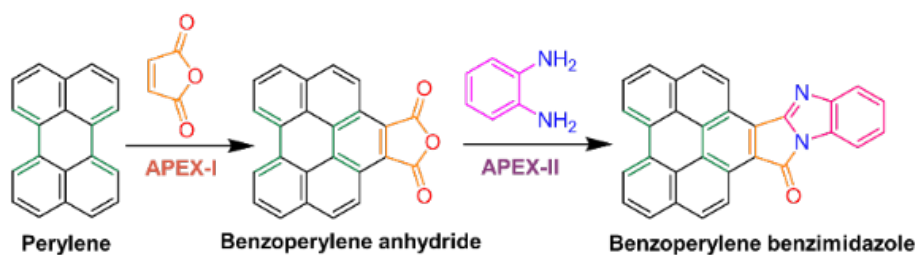
The required reagents are brought from Alfa aesar (*p*-chloranil), TCI (Perylene and Phenyltriboronic acid, tris(pinacol) ester) are used as received. FT-IR spectra were recorded using a JASCO model FT/IR-4600. Solid state ¹³C NMR CP/MAS measurements were performed on Bruker Avance Neo (125 MHz) spectrometer with ¹³C-spin rate 10000 Hz and Probe: Bruker 3.2mm. Electronic absorption spectra were recorded using a JASCO model V-770 UV-VIS-NIR spectrophotometer in a screw-capped quartz cell of 10 mm optical path length. Fluorescence spectra were recorded using a JASCO model FP-8300 spectrometer in a screw capped quartz cell of 10 mm optical path length. Thermogravimetric analysis (TGA) was carried out on TA instrument SDT Q 600 using alumina crucible under nitrogen gas flow rate of 100 mL/min and heating rate 10 °C/min. SEM measurements were performed on a JEOL JIB4700F (FIB-SEM). Surface area measurements were carried out on Quantachrome ASiQwin™. Samples were degassed before the measurement at 150 °C for 12 hrs. Powder XRD patterns of CPPs recorded by Rigaku (Rigaku Ultima IV, Rigaku) with Cu target [Cu Kα1 radiation ($\lambda = 1.54 \text{ \AA}$)] as a radiation source. XPS analysis was carried out on AXIS SUPRA (serial no. C332905/01). pH was calculated by using HANNA instruments (HI 2215) pH ORP meter. DLS analysis was carried out on Nicomp® Nano DLS/ZLS Systems.

2. Computational Details

All the calculations were performed using ORCA 4.2.1. code.^{S1} Solvent-phase geometry optimization was carried out, considering chloroform as the solvent and using the B3LYP^{S2} functional with def2-SVP^{S3} basis set for all the atoms. The DFT optimized geometry of PER, BPA and BPBI are provided in ESI. Dispersion corrections were accounted for by Grimme's Dispersion correction with Becke's-Johnson damping (D3-BJ) scheme^{S4} as implemented in ORCA. To speed up the calculations, here, we have used resolution of identity chain-of-spheres (RIJCOSX) approximation^{S5} as implemented in ORCA. The computation of the numerical Hessian with no negative eigenvalue indicates that the optimized geometries are minima on the potential energy surface. To compute the electronic absorption spectrum of the complexes, we have performed time-dependent density functional theory (TD-DFT) calculations using ORCA 4.2.1 code. The TDDFT calculations were carried out using long-range corrected CAM-B3LYP^{S6} functional with Grimme's dispersion correction and with def2-TZVP(-f) level of basis set^{S3}. In TD-DFT calculations, we have incorporated the solvent effects (chloroform) by implicit Conductor-like Polarizable Continuum Model (CPCM)^{S7}. The full TD-DFT calculations were performed where the Tamm-Dancoff approximation was turned off throughout the calculations.

3. Synthesis:

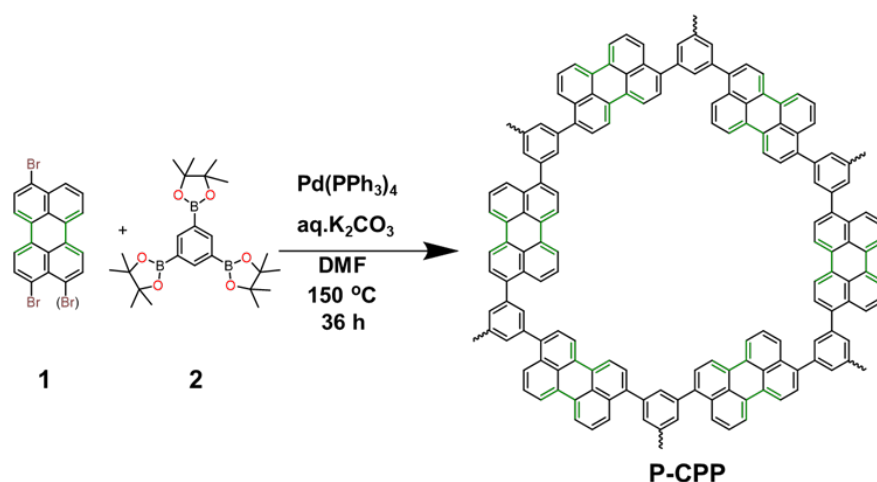
(a) **Scheme S1:** Synthetic scheme for APEX-I and APEX-II reactions on perylene.



(b) **Synthesis of monomer (mixture of 3,9-Dibromoperylene and 3,10-Dibromoperylene).**

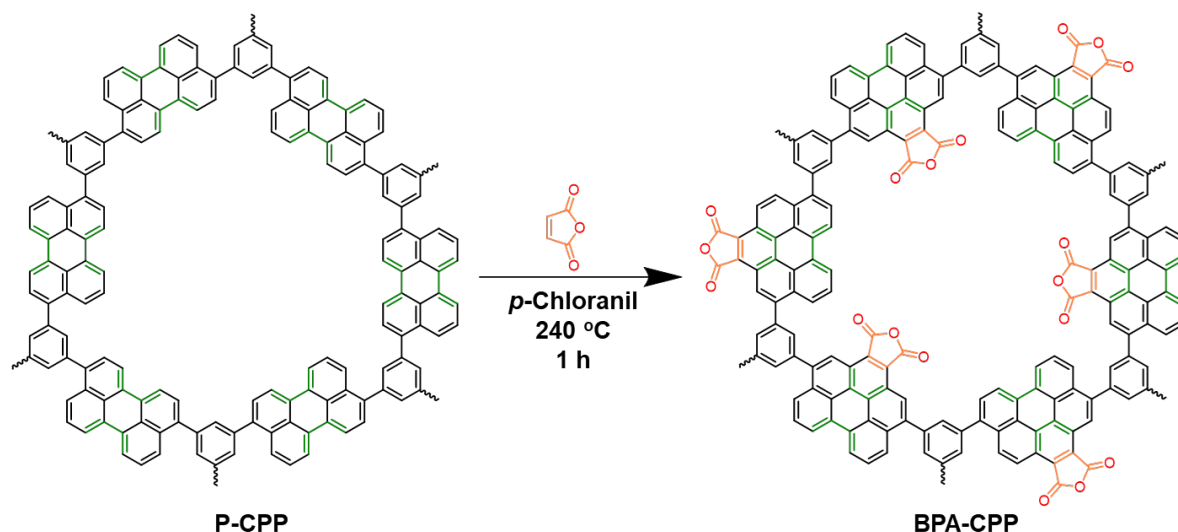
The mixture of 3,9-dibromoperylene and 3,10-dibromoperylene was synthesised according to the reported procedure. ^[S8]

(c) **Synthesis of Perylene based CPP (P-CPP).**



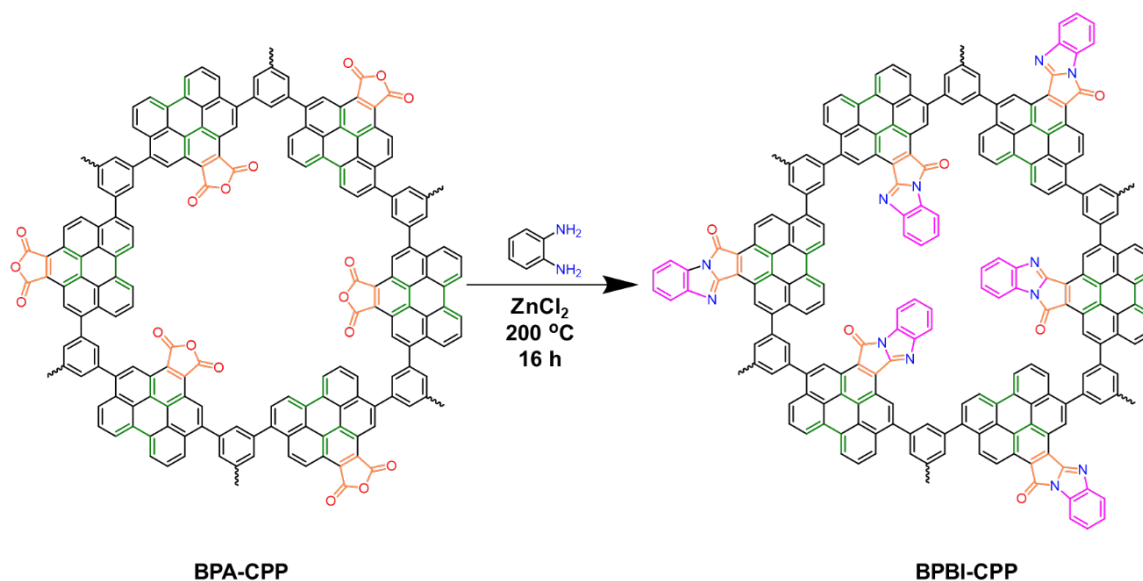
The Schlenk tube was charged with dibromoperylene mixture (1) (134.74 mg, 0.32 mmol), 1,3,5-Phenyltriboronic acid, tris(pinacol) ester (2) (100 mg, 0.21 mmol), K_2CO_3 (2 eq), DMF (15 ml) and water (1.5 ml) and degassed by three freeze–pump–thaw cycles. After that tetrakis(triphenylphosphine)-palladium (0) (37 mg, 0.032 mmol) was added to this mixture. The mixture was again degassed by freeze-pump-thaw cycle and purged with nitrogen gas. The resultant mixture was heated to $150\text{ }^\circ\text{C}$ under stirring for 36 hours. After cooling to room temperature, the mixture was poured into water and filtered and washed with water, methanol and chloroform. Further, it was purified by Soxhlet extraction with methanol and chloroform for 12 hours each. After vacuum drying at $100\text{ }^\circ\text{C}$ P-CPP was obtained as a green powder. Yield: 126 mg. Solid-state ^{13}C NMR (125 MHz, δ ; ppm): 139.41, 129.82, 126.45, 119.86. FTIR (cm^{-1}): 3440.16, 3040.43, 2344.23, 1574.66, 1191.80, 1384.50, 829.11, 809.65, 763.87.

(d) Synthesis of Benzoperylene anhydride CPP (BPA-CPP).



Perylene based CPP (**P-CPP**) (90 mg), *p*-chloranil (473 mg) and maleic anhydride (2.5 g) were charged in a sealed tube and refluxed at 240 °C for 1 hour. After that hot xylene was added to the reaction mixture and filtered. The obtained precipitate was washed with diethyl-ether and acetone. The precipitate was further purified by Soxhlet extraction with methanol, acetone and chloroform solvent for 12 hours each. After vacuum drying at 100 °C, **BPA-CPP** was obtained as a red powder. Yield: 110 mg. Solid-state ^{13}C NMR (125 MHz, δ ; ppm): 162.24, 140.11, 129.00, 123.67. FTIR (cm^{-1}): 3531.39, 2345.86, 1795.45, 1763.08, 1606.66, 1387.90, 1299.82, 1188.24, 899.75.

(e) Synthesis of Benzoperylene benzimidazole CPP (BPBI-CPP).



Benzoperylene anhydride CPP (**BPA-CPP**) (60 mg), o-phenylene-diamine (330 mg) and zinc chloride (20 mg) were taken in quinoline (10 ml) and degassed with nitrogen for 30 min. The reaction mixture was refluxed at $200\text{ }^\circ\text{C}$ for 16 hours under an inert nitrogen atmosphere. After that reaction mixture was allowed to cool to room temperature and water was poured into the mixture and filtered. The precipitate was further purified by Soxhlet extraction with water, methanol and chloroform 12 hours each. After vacuum drying at $100\text{ }^\circ\text{C}$, **BPBI-CPP** was obtained as an orange powder. Yield 92 mg. FTIR (cm^{-1}): 3411.28, 3052.37, 2920.30, 1742.06, 1599.77, 1561.19, 1487.24, 1428.68, 1373.71, 1186.37, 1129.61, 821.27, 747.47.

Solubility of CPPs: We have tested the solubility of the all CPPs in solvents like chloroform, dichloromethane, methanol, tetrahydrofuran, DMF, DMSO and Toluene, and found that they are insoluble. According to our observations it is difficult to find a solvent where these polymers are soluble as they possess crosslinked porous network.

3. Supporting Figures and Tables:

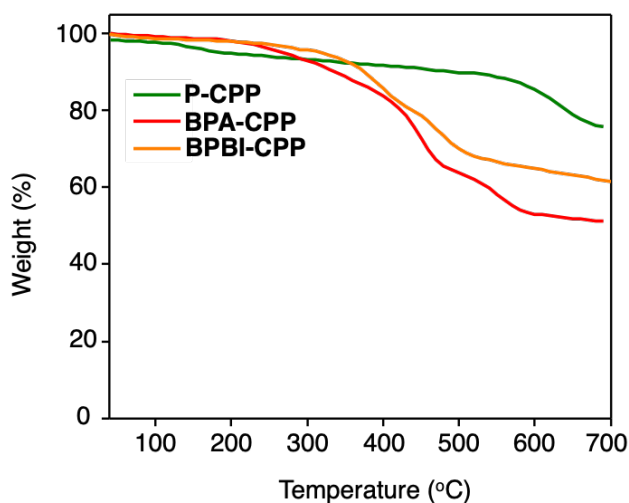


Figure S1. TGA profiles of **P-CPP**, **BPA-CPP** and **BPBI-CPP** measured under nitrogen gas flow of 100 mL/min at a heating rate of 10 °C/min.

P-CPP is stable up to 500 °C with ~10% weight loss (Figure S1). However, **BPA-CPP** start to decompose from above 400 °C. This is could be due to the presence of anhydride group in **BPA-CPP** which is known to decompose above 350 °C.^[S9] In case of **BPBI-CPP**, the slight weight loss from 250 to 400 °C is be due to the decomposition of trapped o-diamino benzene molecules (see main text). From 400-600 °C, the weight loss could be due to the decomposition carbonyl and benzimidazole groups.

Table S1. Specific surface area (SSA) of CPPs, total pore volume and CO₂ uptake of CPPs.

CPPs	Specific surface area (m²/g) at 77 K	Total pore volume (cc/g)	CO₂ Uptake (mmol/g) at 1 bar pressure and 273 K
P-CPP	534	1.12	1.80
BPA-CPP	573	1.21	1.85
BPBI-CPP	76	0.66	1.71

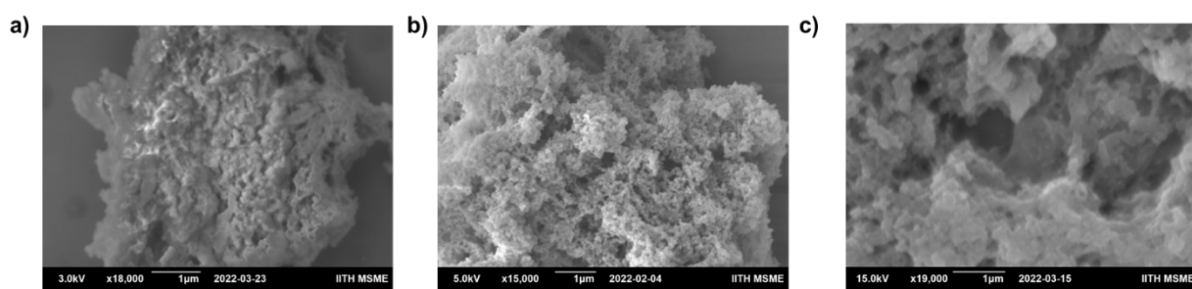


Figure S2. SEM Image of CPPs (a) **P-CPP**, (b) **BPA-CPP** and (c) **BPBI-CPP**.

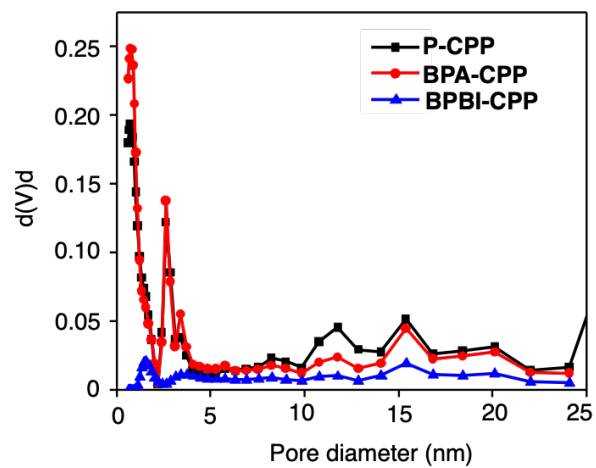


Figure S3. Pore size distribution of all CPPs calculated by QSDFT method.

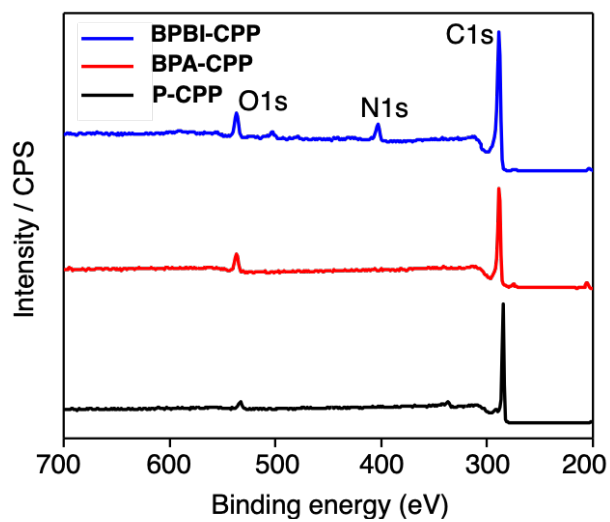


Figure S4. XPS survey spectra of all CPPs. The peak at ~533 eV in **P-CPP** could be due to oxygen atoms from some residual boronate ester functional groups.

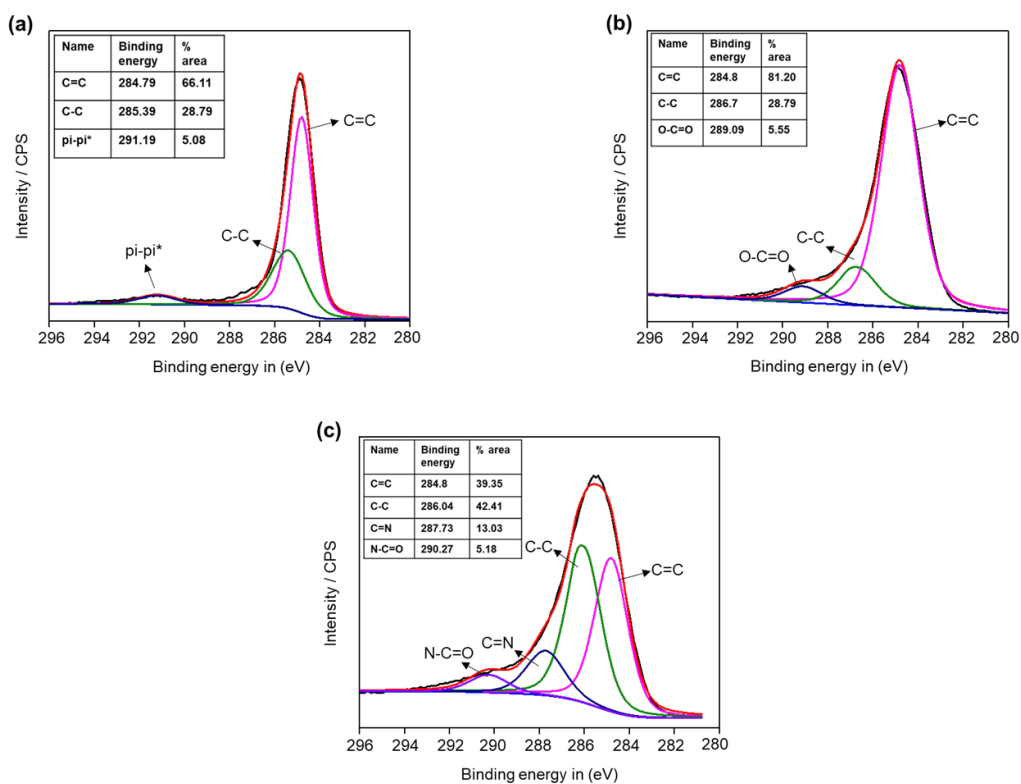


Figure S5. High resolution XPS C1s spectra of (a) **P-CPP**, (b) **BPA-CPP** and (c) **BPBI-CPP**.

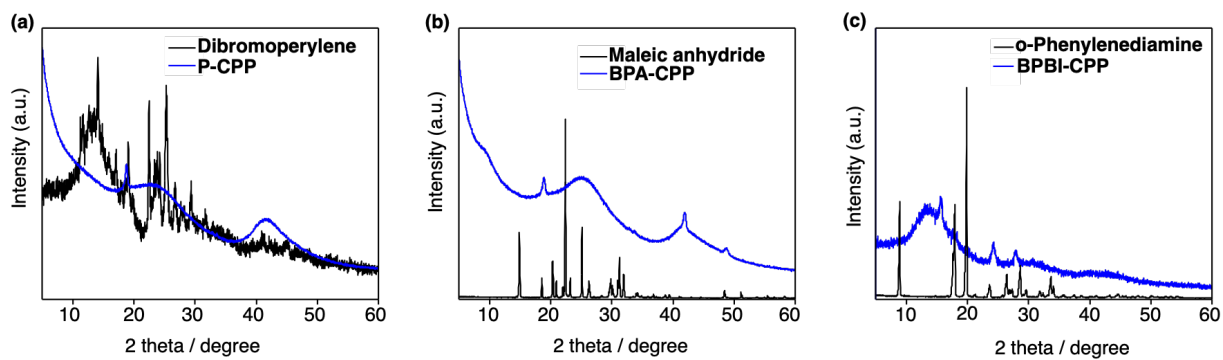


Figure S6. Powder XRD patterns of (a) dibromoperylene (black curve) and **P-CPP** (blue curve). (b) Maleic anhydride (black curve) and **BPA-CPP** (blue curve). (c) o-phenylenediamine (black curve) and **BPBI-CPP** (blue curve).

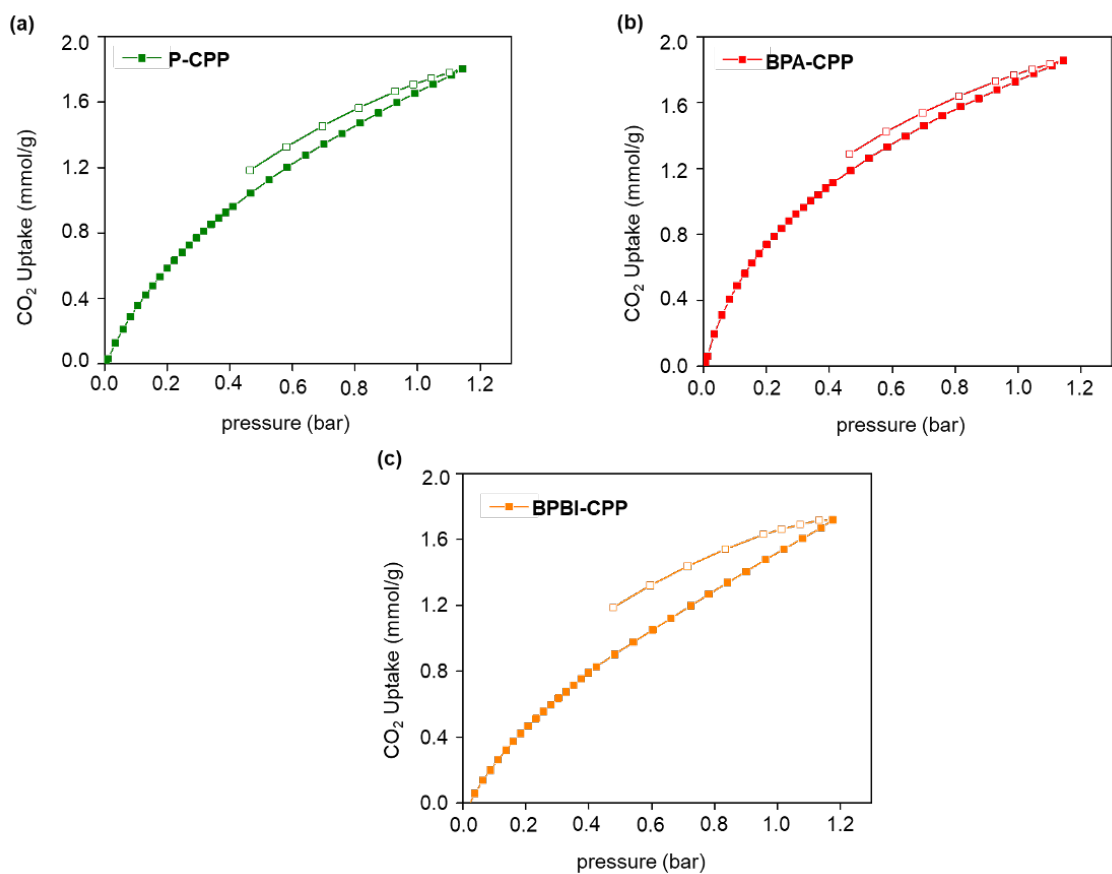


Figure S7. CO₂ Adsorption and desorption isotherms of (a) **P-CPP**, (b) **BPA-CPP** and (c) **BPBI-CPP** up to 1 bar pressure and 273 K temperature.

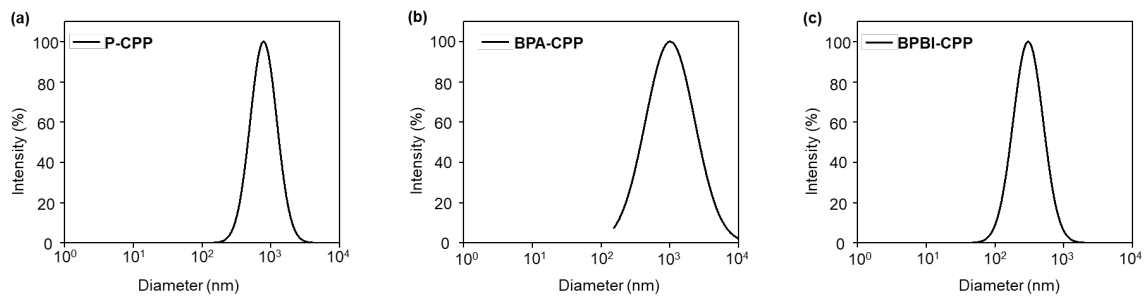


Figure S8. DLS Analysis of (a) **P-CPP** (b) **BPA-CPP** and (c) **BPBI-CPP** dispersed in chloroform.

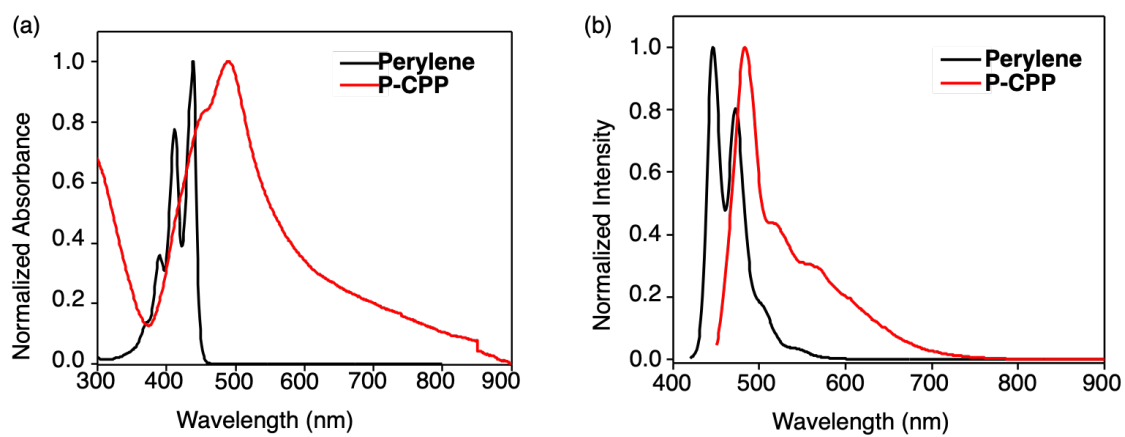


Figure S9. Normalized (a) absorbance and (b) fluorescence spectra of perylene (black) and **P-CPP** (red) in chloroform.

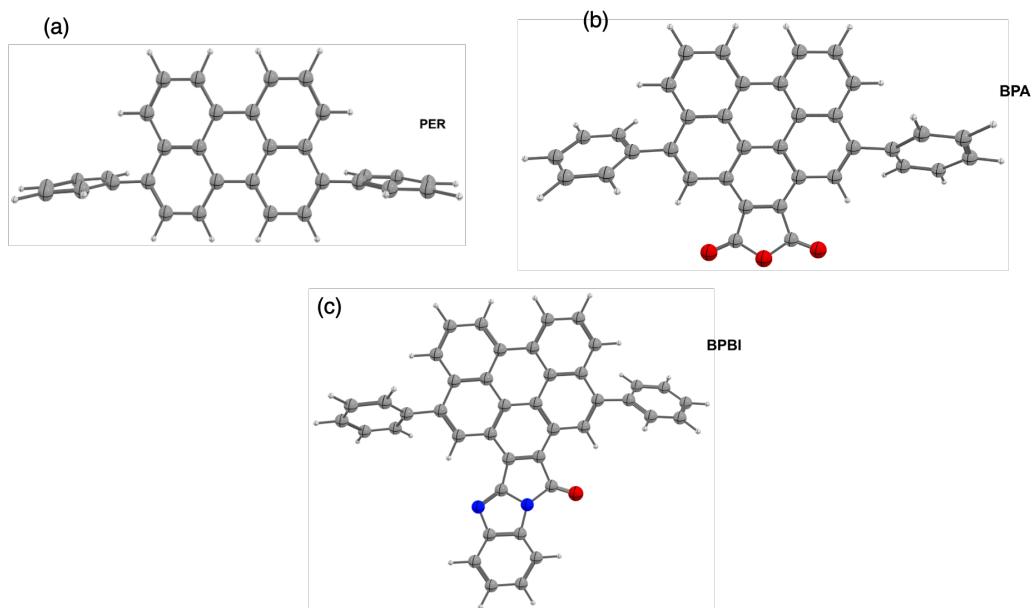


Figure S10. DFT optimized geometries of the model compounds (a) biphenyl perylene (**PER**), (b) biphenyl benzoperylene anhydride (**BPA**) and (c) biphenyl benzoperylene benzimidazole (**BPBI**) used for the calculation of absorption spectra. Color Code: C (grey), N (blue), O (red) and H (white).

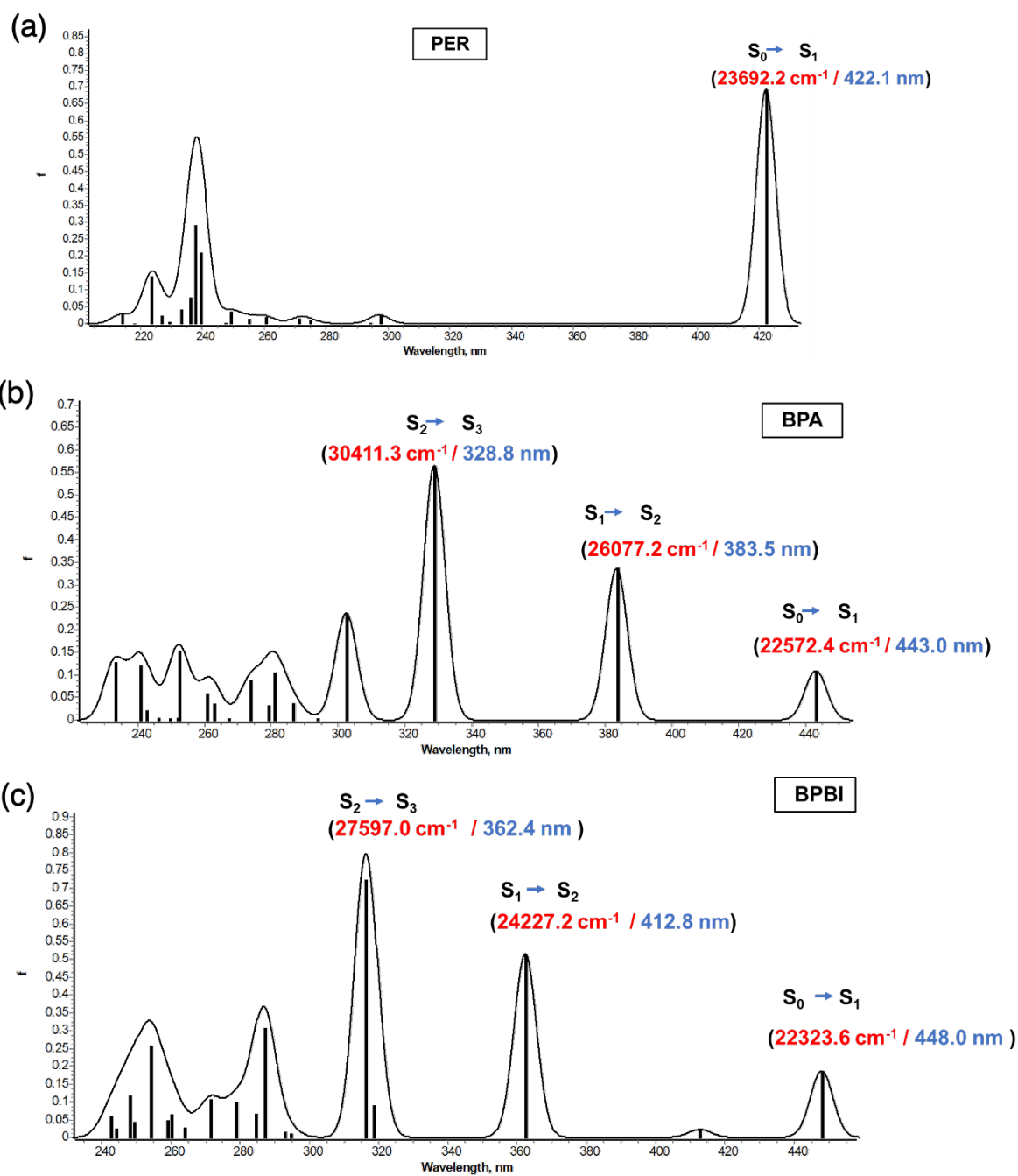


Figure S11. TD-DFT computed absorption spectrum of (a) **PER**, (b) **BPA** and (c) **BPBI** molecules at CAM-B3LYP level of theory.

Table S2. CAM-B3LYP computed vertical excitation energies (in cm^{-1}), corresponding wavelength (nm), nature of frontier molecular orbitals and their contributions along with oscillator strength (f_{osc}) and transition dipole moment for low-lying excited states of **PER**, **BPA** and **BPBI**.

Excited states	E(cm^{-1})	$\lambda(\text{nm})$	Frontier molecular orbitals	% contribution	f_{osc}
PER					
S1	23692.2	422.1	HOMO-LUMO HOMO-1 to LUMO+1	0.98 0.01	0.716
S2	30692.6	325.8	HOMO-LUMO HOMO-1 to LUMO+1	0.77 0.17	0.00003
BPA					
S1	22572.4	443.0	HOMO-LUMO HOMO-1 to LUMO+1	0.91 0.09	0.109
S2	26077.2	383.5	HOMO-LUMO HOMO-1 to LUMO+1	0.84 0.15	0.337
S3	30411.3	328.8	HOMO-LUMO HOMO-1 to LUMO+1	0.82 0.16	0.565
BPBI					
S1	22323.6	448.0	HOMO-LUMO HOMO-1 to LUMO+1	0.91 0.07	0.187
S2	24227.2	412.8	HOMO-LUMO HOMO-1 to LUMO+1	0.78 0.19	0.022
S3	27597.0	362.4	HOMO-LUMO HOMO-1 to LUMO+1	0.82 0.16	0.516

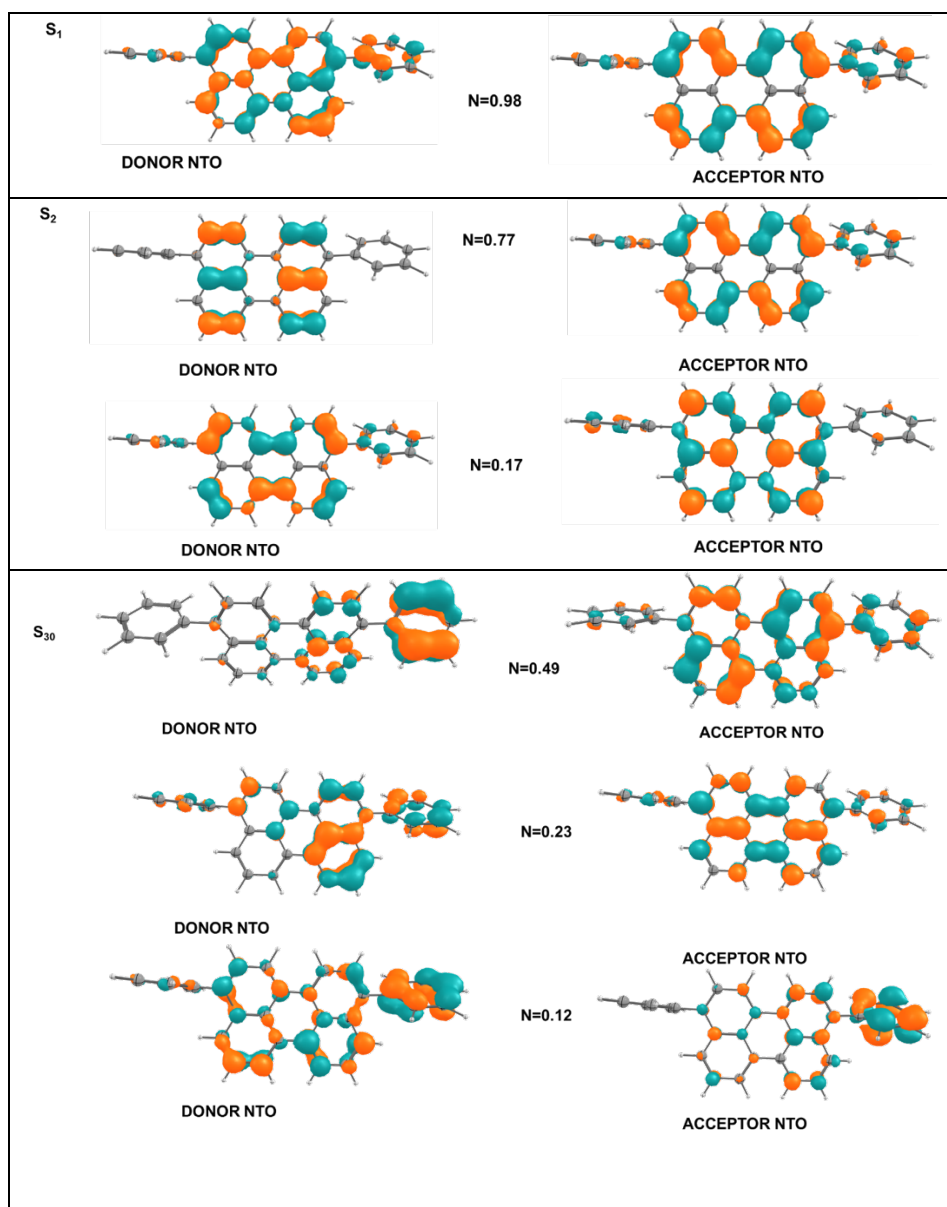


Figure S12: CAM-B3LYP computed NTOs associated with the first three highest oscillator strength electronic excited states of **PER**.

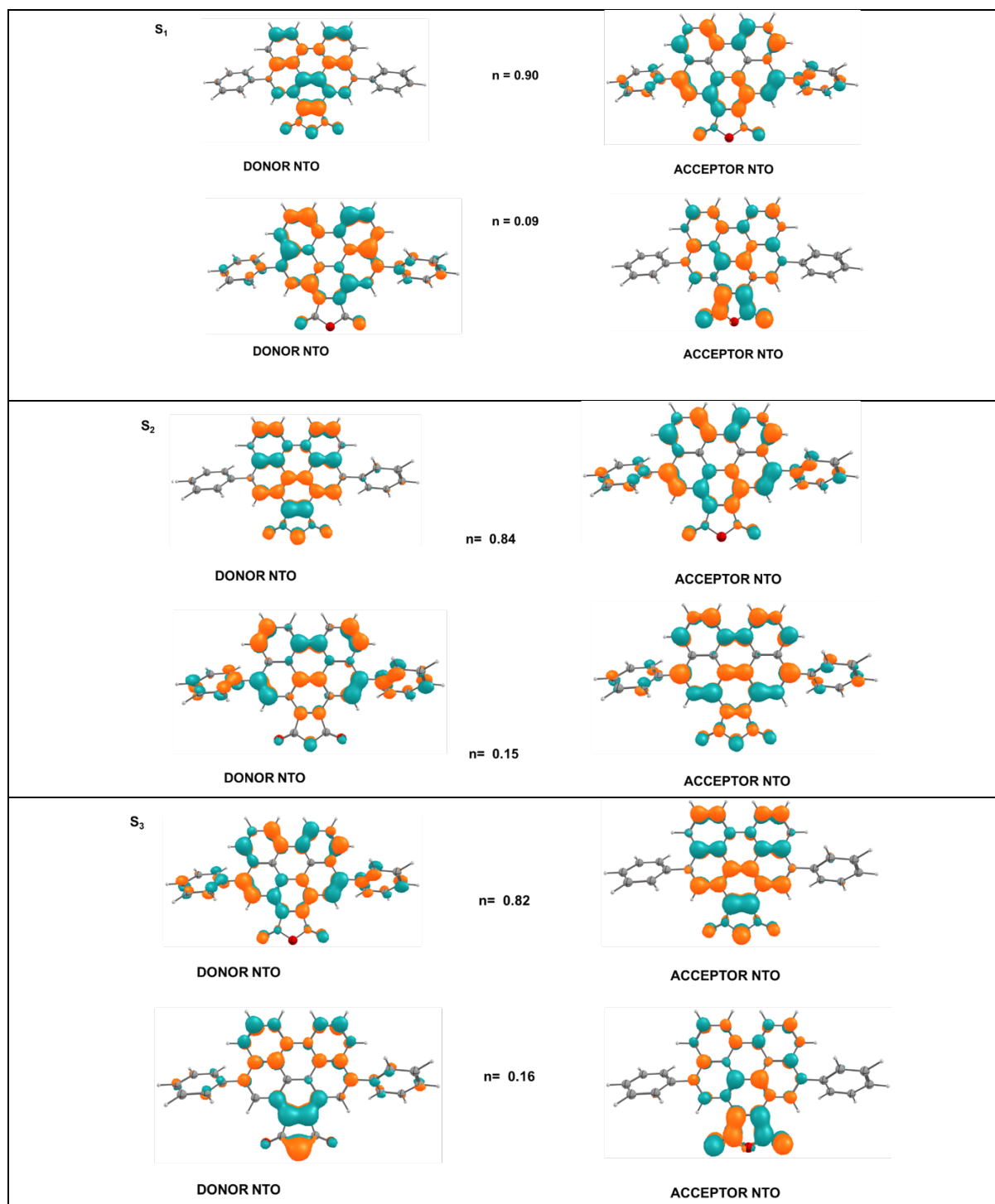


Figure S13. CAM-B3LYP computed NTOs associated with the first three highest oscillator strength electronic excited states of **BPA**.

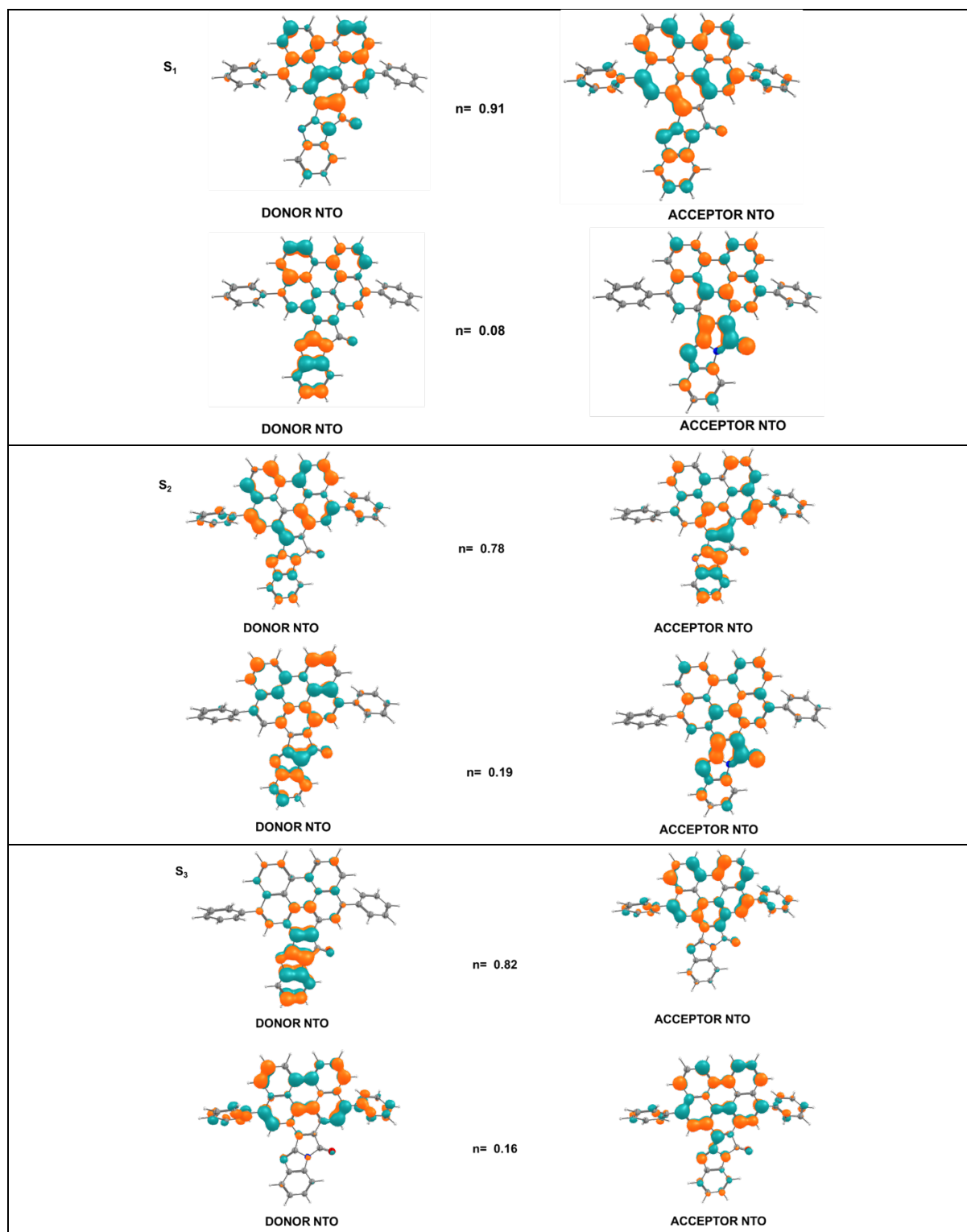


Figure S14. CAM-B3LYP computed NTOs associated with the first three highest oscillator strength electronic excited states of **BPBI**.

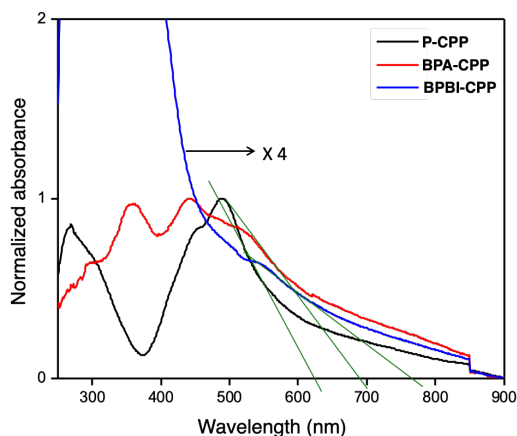


Figure S15. Absorption spectra of CPPs used to calculate optical bandgap (E_{opt}) by drawing a tangent line at with longer wavelength band. The intersecting wavelength of tangent line is used for band gap calculation.

Table S3. Comparison of experimentally calculated band gap of CPPs and theoretically calculated model compounds

CPP	Optical bangap (E_{opt})	Model molecule	Optical bangap (E_{opt})
P-CPP	1.98 eV	PER	2.87 eV
BPA-CPP	1.79 eV	BPA	2.74 eV
BPBI-CPP	1.61 eV	BPBI	2.7 eV

We have calculated the optical band-gap (E_{opt}) for all three CPPs from their longest wavelength absorption band and compared the data with theoretically estimated absorption spectra. For theoretical calculations, we have taken biphenyl perylene (PER), biphenyl benzoperylene anhydride (BPA) and biphenyl benzoperylene benzimidazole (BPBI) as the model compounds (Figure S10). According to the theoretical calculations, the order of the optical band-gap is PER > BPA > BPBI (Figures S11-S14 and Table S3). Experimentally also we have observed similar trend for the corresponding CPPs (Figure S15 and Table S3). After APEX-I and APEX-II reaction, the resultant **BPA-CPP** and **BPBI-CPP** acts like a donor-acceptor polymer. As a result their electronic structure significantly changes which leads to the blue-shift in absorption maxima (Figures S11-S14). However, due to charge-transfer interactions red shifted absorption band between 500-700 nm for **BPA-CPP** and 550-700 nm for **BPBI-CPP** appeared (Figure S15). In case of **BPA-CPP** and **BPBI-CPP** the absorbance of longest wavelength (used for calculating E_{opt}) are weak compared to the other peaks because of their low oscillator strength (Table S2). These red shifted bands are used for calculating E_{opt} as they correspond to S_0 to S_1 transition (Figures S11,15).

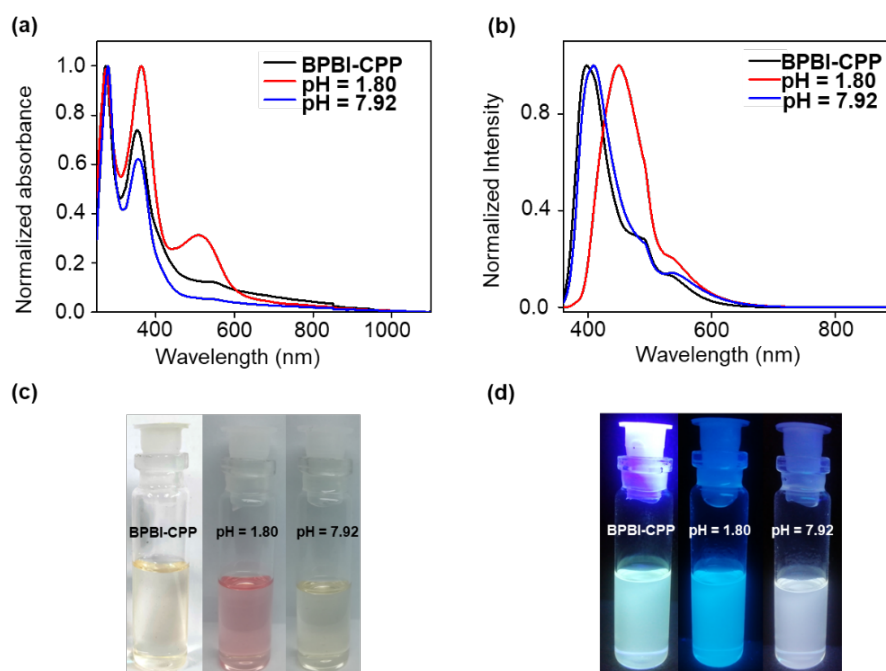


Figure S16. (a) Normalized absorbance and (b) Normalized emission spectra of **BPBI-CPP** (BPBI-CPP (black), acidic (pH = 1.80) (red), neutral (pH = 7.92) (blue). Photographs (c) Under normal light (d) Under UV light. To know the pH of the organic medium, the organic solvent was agitated with water and pH of the water was measured using a pH meter. In the presence of TFA, the pH is found to be 1.80 and triethylamine is added until pH medium is nearly neutral (pH = 7.92).

Since **BPBI-CPP** is endowed with a pH active benzimidazole functional group, we investigated the pH responsive optical properties of **BPBI-CPP** in chloroform using trifluoroacetic acid (TFA) and triethylamine (TEA) as acid and base, respectively (Fig. S16). Under acidic conditions (pH = 1.8), the **BPBI-CPP** solution turned a red color with the appearance of a strong absorption band centered at 512 nm. In addition, the emission maximum was also red shifted to 450 nm compared with the neutral solution, which was at 409 nm (Fig. S16). The changes observed in the optical properties of **BPBI-CPP** after adding TFA could be due to protonation of the imidazole nitrogen of the $-C=N$ bond.^[S10] When this solution was brought back to nearly neutral (pH = 7.9) by adding TEA, the absorption and fluorescence spectra of **BPBI-CPP** resembled those of the initial **BPBI-CPP**. These observations indicate that this process is reversible, and the optical properties and polarity of **BPBI-CPP** can also be tuned *via* the pH as well owing to the imidazole group.

References:

- [S1] Neese, F. The ORCA program system. *WIREs Comput Mol Sci* 2012, 2, 73–78; Neese, F. *WIREs Comput Mol Sci* 2017, e1327.
- [S2] Becke, A. D. *J. Chem. Phys.*, 1993, **98**, 5648-5652.
- [S3] F. Weigend and R. Ahlrichs *Phys. Chem. Chem. Phys.*, 2005, **7**, 3297.
- [S4] (a) S. Grimme, S. Ehrlich, L. Goerigk, *J Comput Chem*, 2011, 32, 1456–1465; (b) S. Grimme, J. Antony, S. Ehrlich and H. Krieg, *J. Chem. Phys.*, 2010, **132**, 154104.
- [S5] (a) R. Izsak, and F. Neese, *Mol. Phys.*, 2013, **111**, 1190–1195; (b) R. Izsak, F. Neese, *J. Chem. Phys.*, 2011, **135**, 144105.
- [S6] T. Yanai, D. P. Tew and N. C. Handy, *Chem. Phys. Lett*, 2004, **393**,51-57
- [S7] (a) A. Klamt, and G. Schüürmann, *J. Chem. Soc., Perkin Trans.* 1993, 799; (b) J. Andzelm, C. Kölmel, A. Klamt, *J. Chem. Phys.* 1995, **103**, 9312–9320; (c) V. Barone and M. Cossi, *J. Phys. Chem. A* 1998, **102**, 1995–2001; (d) M. Cossi, N. Rega, G. Scalmani and V. Barone, *J. Comput. Chem.* 2003, **24**, 669–681.
- [S8] H. Sakaguchi, Y. Kawagoe, Y. Hirano, T. Iruka, M. Yano and T. Nakae, *Adv. Mater.*, 2014, **26** , 4134 –4138.
- [S9] E. Clar and M. Zander *J. Chem. Soc.*, 1957, 4616–4619.
- [S10] H. Sakai, T. Kubota, J. Yuasa, Y. Araki, T. Sakanoue, T. Takenobu, T. Wada, T. Kawai and T. Hasobe, *Org. Biomol. Chem.*, 2016, **14**, 6738.

DFT optimized geometry of PER

C	-0.377641000000	0.094770000000	-3.783139000000
C	-0.292201000000	1.435267000000	-4.116070000000
C	-0.388208000000	-0.326608000000	-2.442697000000
C	-0.209599000000	2.405912000000	-3.068166000000
C	-0.320578000000	0.579999000000	-1.388467000000
C	-0.226363000000	1.976187000000	-1.695170000000
C	-0.460358000000	-1.201372000000	0.365151000000
C	-0.346676000000	0.141674000000	0.017782000000
H	-0.439841000000	-0.651012000000	-4.578971000000
C	-0.470974000000	-1.621473000000	1.703428000000
C	-0.263177000000	1.111602000000	1.068984000000
C	-0.282585000000	0.681320000000	2.444281000000
C	-0.366340000000	-0.719423000000	2.751949000000
H	-0.536770000000	-2.689116000000	1.924256000000
C	-0.294373000000	1.838271000000	-5.552523000000
C	0.911491000000	1.979879000000	-6.257623000000
C	-1.506693000000	2.040714000000	-6.231571000000
C	0.905123000000	2.302756000000	-7.617564000000
C	-1.513565000000	2.363649000000	-7.591535000000
C	-0.307731000000	2.490372000000	-8.287816000000
H	1.857634000000	1.823636000000	-5.733256000000
H	-2.448071000000	1.936213000000	-5.686267000000
H	1.850243000000	2.406964000000	-8.156822000000
H	-2.463675000000	2.517969000000	-8.109812000000
H	-0.313049000000	2.745152000000	-9.350641000000
C	-0.343252000000	-1.240766000000	4.144177000000
C	-1.345372000000	-2.127430000000	4.581887000000
C	0.698702000000	-0.918085000000	5.034156000000
C	-1.312226000000	-2.667439000000	5.870353000000
C	0.733825000000	-1.460517000000	6.320515000000
C	-0.273419000000	-2.334076000000	6.744866000000
H	-2.162516000000	-2.386168000000	3.903809000000
H	1.498829000000	-0.251268000000	4.705008000000
H	-2.104353000000	-3.347185000000	6.195316000000
H	1.555668000000	-1.203421000000	6.993635000000
H	-0.246486000000	-2.758030000000	7.751894000000
C	-0.117391000000	3.793322000000	-3.360742000000
C	-0.152971000000	2.952634000000	-0.647692000000
C	-0.176730000000	2.511587000000	0.762459000000
C	-0.256352000000	1.666741000000	3.468257000000
C	-0.046456000000	4.717551000000	-2.339703000000
C	-0.128857000000	3.425075000000	1.812827000000
C	-0.177364000000	3.007021000000	3.154145000000
C	-0.064287000000	4.299426000000	-0.995863000000
H	-0.104430000000	4.116475000000	-4.402758000000
H	0.025599000000	5.783588000000	-2.569555000000
H	-0.005019000000	5.063095000000	-0.220955000000
H	-0.064923000000	4.493459000000	1.608403000000

H	-0.159080000000	3.754406000000	3.950784000000
H	-0.313384000000	1.355352000000	4.510617000000
H	-0.455332000000	-1.396039000000	-2.244953000000
H	-0.534149000000	-1.964893000000	-0.408491000000

DFT optimized geometry of BPA

C	-0.130501000000	0.079055000000	-3.779040000000
C	-0.185286000000	1.410256000000	-4.107481000000
C	-0.069584000000	-0.356673000000	-2.422159000000
C	-0.175259000000	2.410248000000	-3.054949000000
C	-0.079766000000	0.597778000000	-1.359181000000
C	-0.120407000000	1.993599000000	-1.681665000000
C	-0.011208000000	-1.718893000000	-2.053444000000
C	0.006831000000	-2.126646000000	-0.730833000000
C	-0.035578000000	-1.214912000000	0.344781000000
C	-0.069841000000	0.172384000000	0.010417000000
H	-0.129842000000	-0.678858000000	-4.562360000000
C	-0.090410000000	-1.630483000000	1.707141000000
C	-0.100520000000	1.136180000000	1.069776000000
C	-0.126264000000	0.696475000000	2.436342000000
C	-0.169383000000	-0.723372000000	2.733360000000
H	-0.119933000000	-2.699218000000	1.916872000000
C	-0.314066000000	1.794614000000	-5.539642000000
C	0.613990000000	2.640270000000	-6.174623000000
C	-1.390281000000	1.287916000000	-6.289293000000
C	0.455590000000	2.984983000000	-7.519258000000
C	-1.550403000000	1.636068000000	-7.632828000000
C	-0.632458000000	2.492090000000	-8.248464000000
H	1.468192000000	3.024992000000	-5.612580000000
H	-2.114592000000	0.629826000000	-5.803710000000
H	1.185752000000	3.640776000000	-8.000136000000
H	-2.397557000000	1.239856000000	-8.198183000000
H	-0.765308000000	2.777374000000	-9.295213000000
C	-0.345249000000	-1.232786000000	4.118807000000
C	-1.430784000000	-0.807993000000	4.907128000000
C	0.514444000000	-2.221648000000	4.629124000000
C	-1.653402000000	-1.362992000000	6.168772000000
C	0.294081000000	-2.772549000000	5.894567000000
C	-0.793261000000	-2.348676000000	6.665023000000
H	-2.119254000000	-0.055930000000	4.515092000000
H	1.361592000000	-2.557909000000	4.026482000000
H	-2.507901000000	-1.029867000000	6.763074000000
H	0.973547000000	-3.537871000000	6.278127000000
H	-0.974284000000	-2.788056000000	7.649347000000
C	-0.257213000000	3.787337000000	-3.342236000000
C	-0.126664000000	2.968927000000	-0.635390000000
C	-0.098176000000	2.532884000000	0.764846000000
C	-0.082120000000	1.663233000000	3.459859000000
C	-0.250302000000	4.727612000000	-2.319524000000

C	-0.076722000000	3.448910000000	1.826412000000
C	-0.055663000000	3.018310000000	3.153931000000
C	-0.180961000000	4.325916000000	-0.984772000000
H	-0.335771000000	4.118103000000	-4.376705000000
H	-0.311196000000	5.791292000000	-2.561718000000
H	-0.186933000000	5.091744000000	-0.210267000000
H	-0.064972000000	4.519781000000	1.626804000000
H	-0.017074000000	3.755006000000	3.959366000000
H	-0.057166000000	1.342043000000	4.500661000000
C	0.055857000000	-3.604665000000	-0.712133000000
C	0.029611000000	-2.936044000000	-2.896695000000
O	0.070520000000	-4.031555000000	-2.037252000000
O	0.033586000000	-3.076453000000	-4.086561000000
O	0.077291000000	-4.381786000000	0.199927000000

DFT optimized geometry of BPBI

C	4.021865000000	-0.811287000000	-9.282630000000
C	4.050708000000	0.345557000000	-10.016432000000
C	5.156848000000	-1.248617000000	-8.534442000000
C	5.257798000000	1.151394000000	-10.046073000000
C	6.352071000000	-0.467324000000	-8.515779000000
C	6.398831000000	0.747527000000	-9.274705000000
C	5.153905000000	-2.452431000000	-7.802743000000
C	6.273490000000	-2.882301000000	-7.082433000000
C	7.460881000000	-2.120907000000	-7.032365000000
C	7.493705000000	-0.895516000000	-7.765787000000
H	3.117930000000	-1.421848000000	-9.248971000000
C	8.609647000000	-2.537343000000	-6.295648000000
C	8.682608000000	-0.095027000000	-7.734851000000
C	9.813401000000	-0.518997000000	-6.957308000000
C	9.756622000000	-1.785472000000	-6.250966000000
H	8.564106000000	-3.494904000000	-5.778370000000
C	2.849224000000	0.747453000000	-10.797427000000
C	2.380250000000	-0.070699000000	-11.838321000000
C	2.156135000000	1.934054000000	-10.501224000000
C	1.250211000000	0.294847000000	-12.576768000000
C	1.020475000000	2.292752000000	-11.230977000000
C	0.569056000000	1.478532000000	-12.276210000000
H	2.918434000000	-0.991765000000	-12.075886000000
H	2.508199000000	2.571281000000	-9.686504000000
H	0.901429000000	-0.348075000000	-13.388990000000
H	0.483528000000	3.210813000000	-10.979024000000
H	-0.313906000000	1.766452000000	-12.852487000000
C	10.909328000000	-2.312383000000	-5.472547000000
C	10.719665000000	-2.715418000000	-4.138753000000
C	12.175582000000	-2.498297000000	-6.057290000000
C	11.763505000000	-3.289251000000	-3.410103000000
C	13.219503000000	-3.072705000000	-5.328479000000

C	13.017462000000	-3.470014000000	-4.002041000000
H	9.743335000000	-2.567119000000	-3.671430000000
H	12.334312000000	-2.212679000000	-7.099431000000
H	11.593557000000	-3.601546000000	-2.376385000000
H	14.192414000000	-3.223224000000	-5.803548000000
H	13.833340000000	-3.923264000000	-3.433782000000
C	5.350399000000	2.310788000000	-10.841789000000
C	7.588714000000	1.540521000000	-9.284518000000
C	8.735916000000	1.134307000000	-8.463868000000
C	10.939459000000	0.324396000000	-6.879427000000
C	6.519677000000	3.062145000000	-10.864990000000
C	9.893113000000	1.921826000000	-8.365875000000
C	10.975169000000	1.526175000000	-7.577618000000
C	7.621137000000	2.687196000000	-10.093521000000
H	4.498683000000	2.612991000000	-11.450588000000
H	6.580842000000	3.954369000000	-11.492311000000
H	8.521225000000	3.298717000000	-10.143175000000
H	9.955128000000	2.872308000000	-8.894586000000
H	11.853395000000	2.171948000000	-7.506233000000
H	11.784351000000	0.034885000000	-6.255273000000
C	5.976942000000	-4.205413000000	-6.439091000000
C	4.115249000000	-3.468924000000	-7.632371000000
N	4.653526000000	-4.483285000000	-6.839863000000
N	2.879055000000	-3.683806000000	-7.983018000000
O	6.657010000000	-4.916665000000	-5.734813000000
C	3.660786000000	-5.438862000000	-6.666977000000
C	2.550039000000	-4.913705000000	-7.394397000000
C	1.346648000000	-5.624745000000	-7.429815000000
C	3.607369000000	-6.650384000000	-5.983825000000
C	1.281081000000	-6.837666000000	-6.736308000000
C	2.390449000000	-7.341897000000	-6.031505000000
H	0.491900000000	-5.232122000000	-7.983926000000
H	0.351065000000	-7.410821000000	-6.740991000000
H	2.300570000000	-8.296582000000	-5.507568000000
H	4.470706000000	-7.035740000000	-5.440001000000

SAMPLE INPUT USED FOR TDDFT CALCULATIONS

```
!def2-TZVP(-f) CAM-B3LYP slowconv D3BJ RIJCOSX grid6 gridx6 nofinalgrid
NoFinalGridX
normalprint

!KDIIS

!CPCM(Chloroform)

%maxcore 2048

%pal nprocs 12
end

%scf
maxiter 1000
end

%geom
maxiter 1000
end

%scf
directresetfreq 1
diismaxeq 25
end

%tddft nroots 20
TDA FALSE
DoNTO true
NTOstates 1,2,3,4,5,6
end

*xyz 0 1
DFToptimized coordinates
*
```